

Trajectories and Stability Regions of the Lagrangian Point L_1 in the Generalized Chermnykh-Like Problem

Badam Singh Kushvah

*Department of Applied Mathematics, Indian School of Mines
Dhanbad-826009,INDIA,Phone:+91-326-2235765,Fax:+91-326-2296563*

Abstract

The Lagrange point L_1 for the Sun-Earth system is considered due to its special importance for the scientific community for the design of space missions. The location of the Lagrangian points with the trajectories and stability regions of L_1 are computed numerically for the initial conditions very close to the point. The influence of belt, effect of radiation pressure due to Sun and oblateness effect of second primary (finite body Earth) is presented for various values of parameters. The collinear point L_1 is asymptotically stable within a specific interval of time t correspond to the values of parameters and initial conditions.

Keywords: trajectory, stability, equilibrium points, radiation pressure, oblateness, rtbp.

2008 MSC: code, 70F15

1. Introduction

The circular restricted three body problem is modification of the three body problem where the third body is assumed to have very small mass which is infinitesimal in comparison to other two finite masses are called primaries. The restricted three body problem is generalized to include radiation pressure, oblateness of the second primary and influence of the belt. Further the

Email address: bskush@gmail.com, kushvah.bs.am@ismdhanbad.ac.in (Badam Singh Kushvah)

URL: <http://www.ismdhanbad.ac.in/depart/math/faculty1.htm> (Badam Singh Kushvah)

primary bodies are moving in circular orbits about their center of mass. The well-known five equilibrium points(Lagrangian points) that appear in the planar restricted three-body problem are very important for astronomical applications. The collinear points are unstable and the triangular points are stable Szebehely [1]. In the Sun-Jupiter system several thousand asteroids, collectively referred to as Trojan asteroids, are in orbits of triangular equilibrium points. But collinear equilibrium points are also made linearly stable by continuous corrections of their orbits(“halo orbits”). In other words the collinear equilibrium points are metastable points in the sense that, like a ball sitting on top of a hill. However, in practice these Lagrange points have proven to be very useful indeed since a spacecraft can be made to execute a small orbit about one of these Lagrange points with a very small expenditure of energy Farquhar [2, 3]. Because of the its unobstructed view of the Sun, the Sun-Earth L_1 is a good place to put instruments for doing solar science. NASA’s Genesis Discovery Mission has been there, designed completely using invariant manifolds and other tools from dynamical systems theory. In 1972, the International Sun-Earth Explorer (ISEE) was established , joint project of NASA and the European Space Agency(ESA). The ISEE-3 was launched into a halo orbit around the Sun-Earth L_1 point in 1978, allowing it to collect data on solar wind conditions upstream from the Earth Farquhar et al. [4]. In the mid-1980s the Solar and Heliospheric Observatory (SOHO) Domingo et al. [5] is places in a halo orbit around the Sun-Earth L_1 position, about a million miles the Sun ward from the Earth. They have provided useful places to “park” a spacecraft for observations.

The Chermnykh’s problem is a new kind of restricted three body problem which was first time studied by Chermnykh [6]. This problem generalizes two classical problems of Celestial mechanics: the two fixed center problem and the restricted three body problem. This gives wide perspectives for applications of the problem in celestial mechanics and astronomy. The importance of the problem in astronomy has been addressed by Jiang and Yeh [7]. Some planetary systems are claimed to have discs of dust and they are regarded to be young analogues of the Kuiper Belt in our Solar System. If these discs are massive enough, they should play important roles in the origin of planets’orbital elements. Since the belt of planetesimal often exists within a planetary system and provides the possible mechanism of orbital circularization, it is important to understand the solutions of dynamical systems with the planet-belt interaction. Chermnykh’s problem has been studied by many scientists such as Papadakis [8], Jiang and Yeh [9], Yeh and Jiang [10],

Papadakis and Kanavos [11] and reference their in.

The goal of present paper is to investigate the nature of collinear equilibrium point L_1 because of the interested point to the mission design. Although there are two new equilibrium points due to mass of the belt (larger than 0.15) Jiang and Yeh [12], Yeh and Jiang [10] but they are left to examine. All the results are computed numerically with the help of computer because pure analytical methods are not suitable. The actual trajectories and the stability regions of L_1 however is more complicated than the discussed here. But for specific the time intervals, and initial values, these results provide new information on the behavior of trajectories around the Lagrangian point L_1 for different possible set values of the parameters.

2. Location of Lagrangian Points

It is supposed that the motion of an infinitesimal mass particle is influenced by the gravitational force from primaries and a belt of mass M_b . The units of the mass, the distance and the time are taken such that sum of the masses and the distance between primaries are unities, the unit of the time i.e. the time period of m_1 about m_2 consists of 2π units such that the Gaussian constant of gravitational $\mathbf{k}^2 = 1$. Then perturbed mean motion n of the primaries is given by $n^2 = 1 + \frac{3A_2}{2} + \frac{2M_b r_c}{(r_c^2 + T^2)^{3/2}}$, where $T = \mathbf{a} + \mathbf{b}$, \mathbf{a}, \mathbf{b} are flatness and core parameters respectively which determine the density profile of the belt, $r_c^2 = (1 - \mu)q_1^{2/3} + \mu^2$, $A_2 = \frac{r_e^2 - r_p^2}{5r^2}$ is the oblateness coefficient of m_2 ; r_e, r_p are the equatorial and polar radii of m_2 respectively, $r = \sqrt{x^2 + y^2}$ is the distance between primaries and $x = f_1(t), y = f_2(t)$ are the functions of the time t i.e. t is only independent variable. The mass parameter is $\mu = \frac{m_2}{m_1 + m_2}$ (9.537×10^{-4} for the Sun-Jupiter and 3.00348×10^{-6} for the Sun-Earth mass distributions respectively), $q_1 = 1 - \frac{F_p}{F_g}$ is a mass reduction factor and F_p is the solar radiation pressure force which is exactly apposite to the gravitational attraction force F_g . The coordinates of m_1, m_2 are $(-\mu, 0), (1 - \mu, 0)$ respectively. In the above mentioned reference system and Miyamoto and Nagai [13] model, the equations of motion of the infinitesimal mass particle in the xy -plane formulated as [please see Kushvah [14, 15]]:

$$\ddot{x} - 2ny \dot{y} = \Omega_x, \quad (1)$$

$$\ddot{y} + 2n\dot{x} = \Omega_y, \quad (2)$$

where

$$\begin{aligned}
\Omega_x &= n^2 x - \frac{(1-\mu)q_1(x+\mu)}{r_1^3} - \frac{\mu(x+\mu-1)}{r_2^3} - \frac{3\mu A_2(x+\mu-1)}{2r_2^5} \\
&\quad - \frac{M_b x}{(r^2 + T^2)^{3/2}} \\
\Omega_y &= n^2 y - \frac{(1-\mu)q_1 y}{r_1^3} - \frac{\mu y}{r_2^3} - \frac{3\mu A_2 y}{2r_2^5} \\
&\quad - \frac{M_b y}{(r^2 + T^2)^{3/2}} \\
\Omega &= \frac{n^2(x^2 + y^2)}{2} + \frac{(1-\mu)q_1}{r_1} + \frac{\mu}{r_2} + \frac{\mu A_2}{2r_2^3} + \frac{M_b}{(r^2 + T^2)^{1/2}} \quad (3) \\
r_1 &= \sqrt{(x+\mu)^2 + y^2}, r_2 = \sqrt{(x+\mu-1)^2 + y^2}.
\end{aligned}$$

From equations (1) and (2), the Jacobian integral is given by:

$$E = \frac{1}{2} (\dot{x}^2 + \dot{y}^2) - \Omega(x, y, \dot{x}, \dot{y}) = (\text{Constant}) \quad (4)$$

which is related to the Jacobian constant $C = -2E$. The location of three collinear equilibrium points and two triangular equilibrium points is computed by dividing the orbital plane into three parts $L_1, L_4(5)$: $\mu < x < (1-\mu)$, L_2 : $(1-\mu) < x$ and L_3 : $x < -\mu$. For the collinear points, an algebraic equation of the fifth degree is solved numerically with initial approximations to the Taylor-series as:

$$x(L_1) = 1 - \left(\frac{\mu}{3}\right)^{1/3} + \frac{1}{3}\left(\frac{\mu}{3}\right)^{2/3} - \frac{26\mu}{27} + \dots \quad (5)$$

$$x(L_2) = 1 + \left(\frac{\mu}{3}\right)^{1/3} + \frac{1}{3}\left(\frac{\mu}{3}\right)^{2/3} - \frac{28\mu}{27} + \dots \quad (6)$$

$$x(L_3) = -1 - \frac{5\mu}{12} + \frac{1127\mu^3}{20736} + \frac{7889\mu^4}{248832} + \dots \quad (7)$$

$$(8)$$

The solution of differential equations (1) and (2) is presented as interpolation function which is plotted for various integration intervals by substituting specific values of the time t and initial conditions i.e. $x(0) = x(L_i), y(0) = 0$

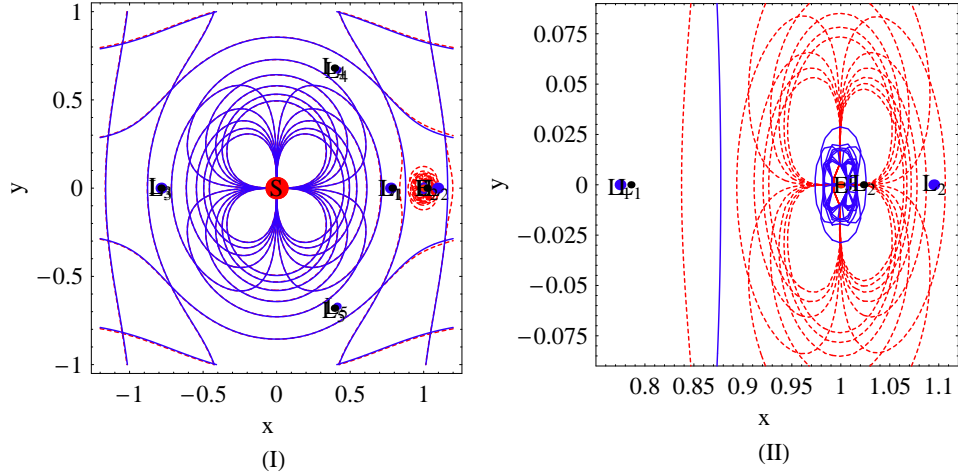


Figure 1: The position of equilibrium points when $T=0.01$, $q_1 = 0.75$, $A_2 = 0.05$ and $M_b = 0.4$, panel (I):Red dotted curves and blue points for Sun-Jupiter mass distribution, blue curves and black points for Sun-Earth mass distribution, (II): Position of L_1, L_2 with respect to Jupiter's and Earth's is shown in zoom

where $i = 1 - -3$ and $x(0) = \frac{1}{2} - \mu$, $y(0) = \pm \frac{\sqrt{3}}{2}$ for the triangular equilibrium points. The equilibrium points are shown in figure 1 in which two panels i.e. (I) red solid curves and blue points correspond to the Sun-Jupiter mass distribution and blue dashed curves and black points correspond to the Sun-Earth mass distribution. Panel (II) show the zoom of the neighborhood of L_1, L_2 . The numerical values of these points are presented in Table 1. One can see that the positions of L_1, L_3 appeared rightward and the positions of L_2, L_4 (L_4 is shifted downward also) are shifted leftward in the Sun-Earth system with respect to the position in the Sun-Jupiter system. The nature of the L_5 is similar to the L_4 . The detail behavior of the L_1 with stability regions is discussed in sections. 3 & 4.

3. Trajectory of L_1

The equations (1-2) with initial conditions $x(0) = x(L_1)$, $y(0) = 0$, $x'(0) = y'(0) = 0$ are used to determine the trajectories of L_1 for different possible cases. The origin of coordinate axes is supposed to the equilibrium point at time $t = 0$ to draw the figures which show the trajectories of

Table 1: Location of equilibrium points when $T=0.01$, $q_1 = .75$, $A_2 = .05$ and $M_b = 0.4$

Sun-Jupiter			Sun-Earth	
L_i	x	y	x	y
L_1	0.774577	0	0.78569	0
L_2	1.09493	0	1.0232	0
L_3	-0.786195	0	-0.785732	0
L_4	0.410603	0.669308	0.393072	0.680342

the point in consideration. They are shown in figure 2 with six panels i.e the panels (I-III) show the trajectory moves about the origin (L_1 at $t = 0$) with $x \in (0.990093, 1.00916)$, $y \in (-0.0061448, 0.00587171)$, the energy $E \in (-12706.5(t = 22.66), -5.08226(t = 0))$ and the distance $r(t) \in (0.990093(t = 0), 1.00916(t = 55))$. The panels (I-III:127 < t < 129.6) show the trajectory moves away from the origin (L_1 at $t = 0$) after a certain value of the time t , with $x \in (0.990093, 1.00916)$, $y \in (-0.0061448, 0.00587171)$, minimum energy $E = -1447$ found at the time $t = 128.52$, and the energy $E > 0$ for $t > 128.88$.

Figure 3 is plotted for $q_1 = 1$, $M_b = 0$ and $A_2 = 0.05$ with six panels (I-III: $0 \leq t \leq 0.06$) and (IV-VI: $0.06 \leq t \leq 1$) which describe the effect of oblateness of Earth to the trajectory of L_1 . The graphs plotted against time which describe behavior of trajectories to equilibrium points not the point itself is moving with time. $x = -1.91954 \times 10^{-48}(t = 0.06)$ to $x = 0.99405(t = .05)$ coordinate y is deceasing function of time that reach maxima -0.0000530614 , at $t = 0.04$ and minima -0.000105662 at time $t = 0.05$ again it deceases and reach at value $-2.5677 \times 10^{47}(t = 0.06)$. Initially energy has negative values for time $0 \leq t < 0.059$ decreases with time t which attains minimum value $-2.64032 \times 10^6(t = 0.059)$ then strictly increasing function that attains positive values after time $t = 0.0594$. In time interval (0.2, 0.6) energy one time returns down that again it tend to very large (infinite) positive value. It is clear from panels (IV-VI) the trajectory move far from the Lagrangian point L_1 after time $t = 0.0594$. The distance $r(t)$ from this point to the trajectory is increasingly periodic for time $0 < t < 0.6$ then tend to very large.

The effect of radiation pressure, oblateness and mass of the belt is considered in figure 4, panels (I&III) describe the trajectory and panels (II&IV) show the energy with respect to the time t . The mass reduction factor

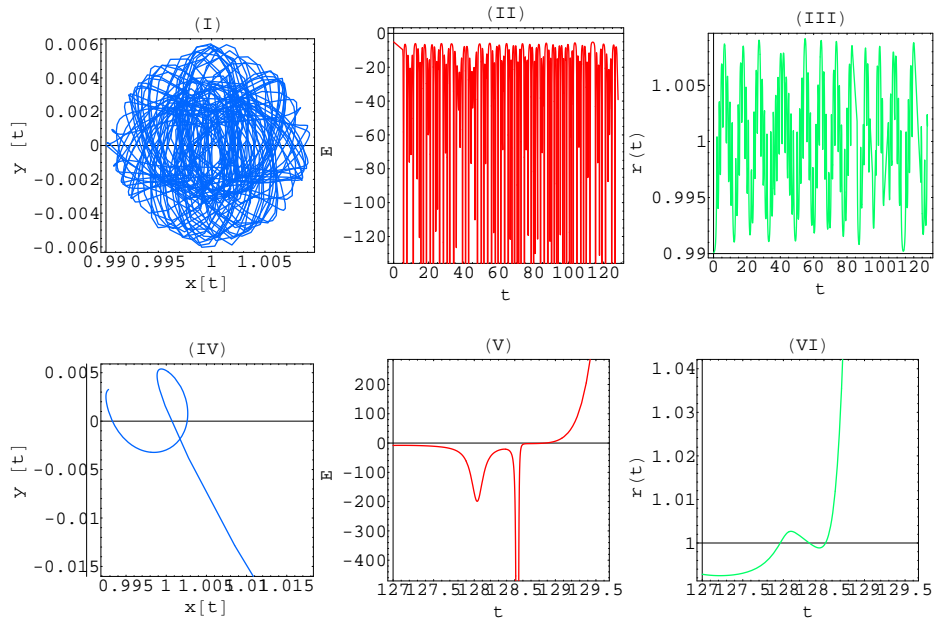


Figure 2: The Panels (I-III): $0 < t < 128.23$ and (IV-VI): $127 < t < 129.6$ in which (I and II) show the trajectory of L_1 , (II and V) show energy-versus time and (III-VI) show the local distance of trajectory at time t from the initial points i.e. $t = 0$ the other parameters are $T=0.01$, $q_1 = 1$, $A_2 = 0$ and $M_b = 0$.

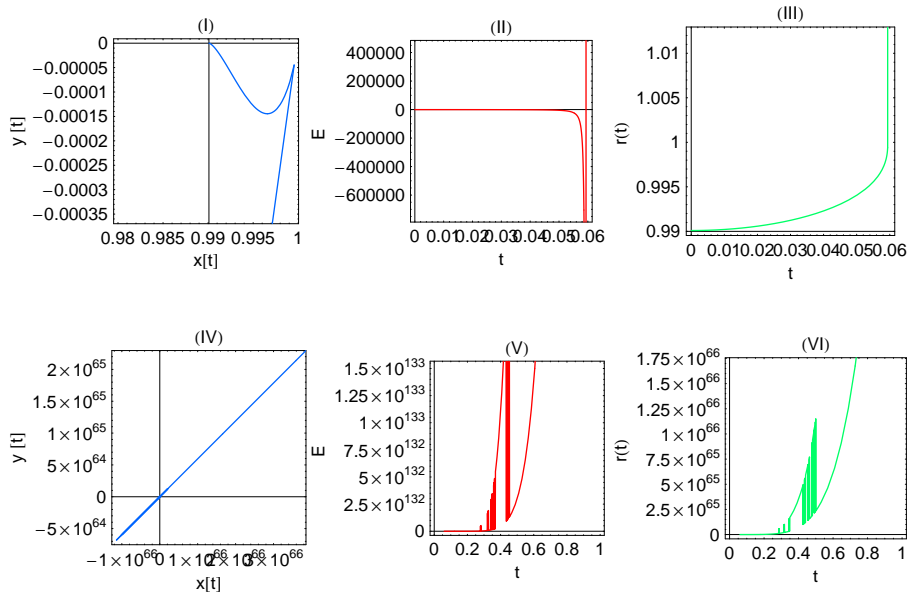


Figure 3: The Panels (I-III): $0 < t < 0.06$ and (IV-VI): $0.06 < t < 1$ in which (I and II) show the trajectory of L_1 , (II and V) show energy-versus-time and (III-VI) show the local distance of trajectory at time t from the initial points i.e. $t = 0$ the other parameters are $T=0.01$, $q_1 = 1$, $A_2 = 0.05$ and $M_b = 0$.

Table 2: Trajectory of L_1 and the energy when $T = 0.01$, $q_1 = .75$, $M_b = 0.2$

A_2	time t	x	y	Energy E
0.25	0.000	0.990093	-1.27593×10^{-32}	-3946.49
	0.002	0.990333	-4.4421×10^{-7}	-4460.93
	0.004	0.991106	-3.63139×10^{-6}	-6764.39
	0.006	0.992646	-1.26827×10^{-5}	-17501.7
	0.008	0.996301	-285308×10^{-5}	-544626.
	0.010	4.03799×10^{55}	-1.06467×10^{54}	7.84745×10^{117}
0.50	0.000	0.990093	7.51113×10^{-33}	-7887.36
	0.002	0.99058	-9.7398×10^{-7}	-10146.9
	0.004	0.992298	-8.12979×10^{-6}	-27763.1
	0.006	-8.35666×10^{48}	-1.70025×10^{47}	2.17394×10^{107}
	0.008	-3.05605×10^{56}	-6.21786×10^{54}	2.74317×10^{119}
	0.010	-9.05111×10^{57}	-1.84154×10^{56}	6.20464×10^{121}
0.75	0.000	0.990093	-1.80556×10^{-34}	-11828.2
	0.002	0.990836	-1.58382×10^{-6}	-17463.6
	0.004	0.993821	-1.33765×10^{-5}	-125336.
	0.006	6.67303×10^{55}	1.19389×10^{54}	4.20091×10^{118}
	0.008	1.02535×10^{58}	1.83448×10^{56}	1.32379×10^{122}
	0.010	1.19678×10^{59}	2.1412×10^{57}	6.74915×10^{123}

$q_1 = 0.75$ and $M_b = 0.2$ are taken to plot the graphs variation in values of these parameters have similar effect. In the panels, solid blue lines represent $A_2 = 0.25$, red dashed lines correspond to $A_2 = 0.50$ and dotted black lines for $A_2 = 0.75$. One can see that the trajectory move very far from the L_1 the energy is positive after a certain value of the time t . Details of trajectory and energy is presented in Table 2 for various values of parameters. One can see that x is an increasing function of the time but y is an initially decreasing function for certain values of the time, then it becomes a strictly increasing. Similarly the energy E is negative and went downward but after some specific the time for each cases it becomes positive and strictly increasing and attains very large positive value.

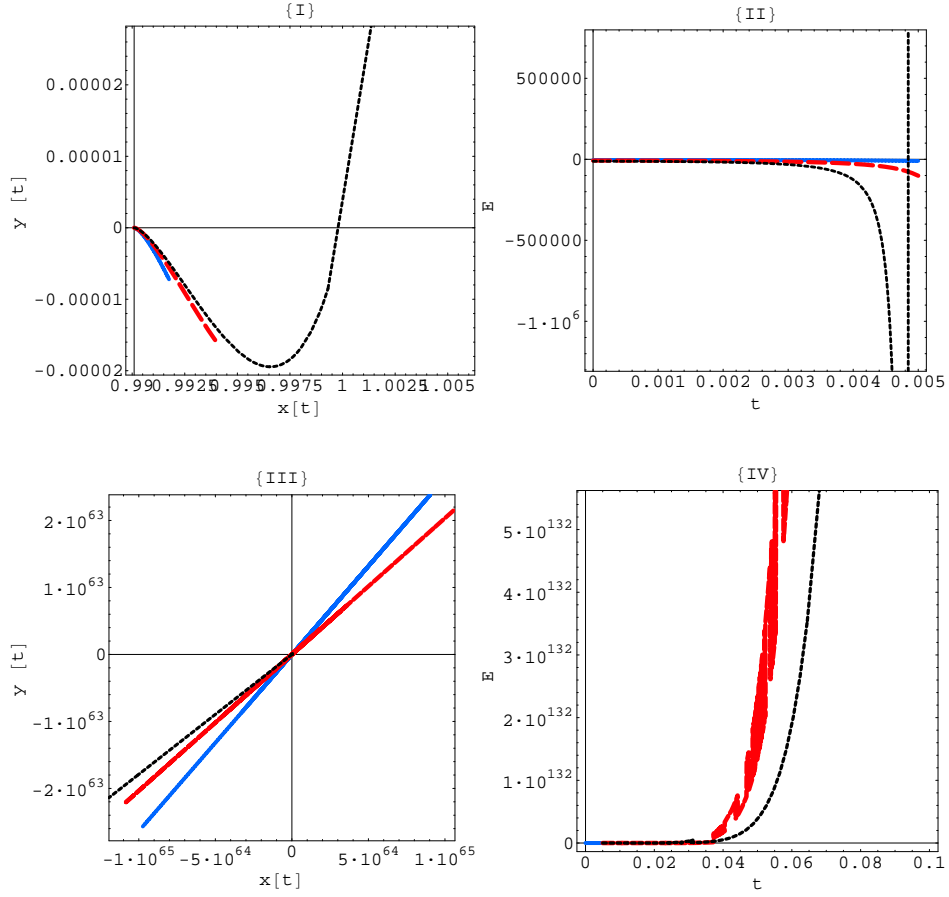


Figure 4: The Panels (I-III): $0 < t < 0.005$ and (II-IV): $0 < t < 1$ in which (I and II) show the trajectory of L_1 , (II and V) show energy-versus time and (III-VI) show the local distance of trajectory at time t from the initial points i.e. $t = 0$ the other parameters are $T=0.01$, $q_1 = 1$, $A_2 = 0.05$ and $M_b = 0$

4. Stability of L_1

Suppose the coordinates (x_1, y_1) of L_1 are initially perturbed by changing $x(0) = x_1 + \epsilon \cos(\phi), y(0) = y_1 + \epsilon \sin(\phi)$ where $\phi = \arctan\left(\frac{y(0)-y_1}{x(0)-x_1}\right) \in (0, 2\pi), 0 \leq \epsilon = \sqrt{(x(0)-x_1)^2 + (y(0)-y_1)^2} < 1$. The ϕ indicates the direction of the initial position vector in the local frame. If the $\epsilon = 0$ means there is no perturbation. It is supposed that the $\epsilon = 0.001$ and the $\phi = \frac{\pi}{4}$ to examine the stability of L_1 . Figure 5 show the path of test particle and its energy with four panels i.e. the panels (I&III): $q_1 = 0.75, 0.50, A_2 = 0.0$, in (I) trajectory of perturbed L_1 moves in chaotic-circular path around initial position without deviating far from it, then steadily move out of the region. In (III) the test particle move in stability region and returns repeatedly on its initial position. The blue solid curves represent $M_b = 0.25$ and dashed curves represent $M_b = 0.50$. It is clear from panel (III) that bounded region for $M_b = 0.25$ is $t < 2500$ and for $M_b = 0.50, t < 2600$.

The effect of oblateness of the second primary is shown in figure 6 when $q_1 = 0.75, M_b = 0.25$. The panel (I) shows the trajectory of perturbed point L_1 and (II) shows the energy of that point. The blue dotted lines correspond to $A_1 = 0.25$ and red lines for $A_2 = 0.50$. One can see that the oblate effect is very powerful on the trajectory and stability of L_1 . When $A_2 = 0.0$ the L_1 is asymptotically stable for the value of t which lies within a certain interval. But if oblate effect of second primary is present ($A_2 \neq 0$), the stability region of L_1 disappears when this effect is increases. Further all the results presented in the manuscripts are similar to the results obtained by [16], Kushvah [17].

5. Conclusion

The numerical computation presented in the manuscript provides remarkable results to design trajectories of Lagrangian point L_1 which helps us to make comments on the stability(asymptotically) of the point. We obtained the intervals of the time where trajectory continuously moves around the L_1 , does not deviate far from the point but tend to approach (for some cases) it, the energy of perturbed point is negative for these intervals, so we conclude that the point is asymptotical stable. More over we have seen that after the specific time intervals the trajectory of perturbed point depart from the neighborhood and goes away from it, in this case the energy also becomes positive, so the Lagrangian point L_1 is unstable. Further the trajectories and

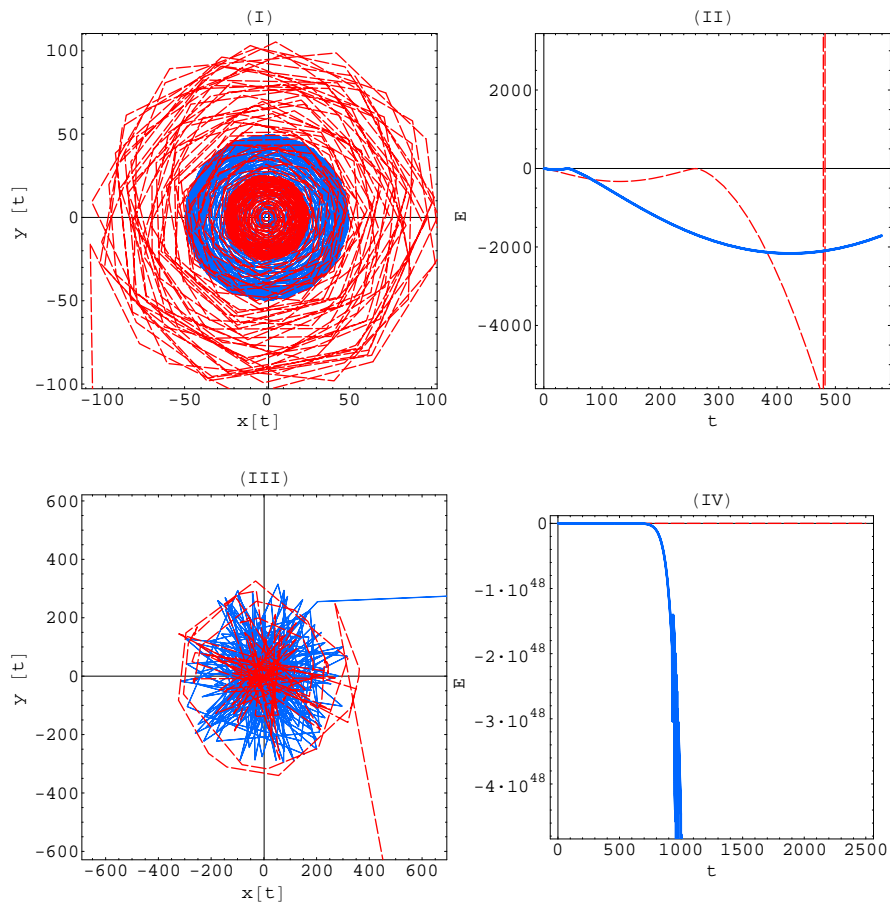


Figure 5: Show the stability of L_1 with panels (I-II): $0 \leq t \leq 491, q_1 = 0.75, A_2 = 0.0$ and (III-IV): $0 < t < 2500, q_1 = 0.50, A_2 = 0.0$ in which blue solid curves for $M_b = 0.25$, red curves for $M_b = 0.50$

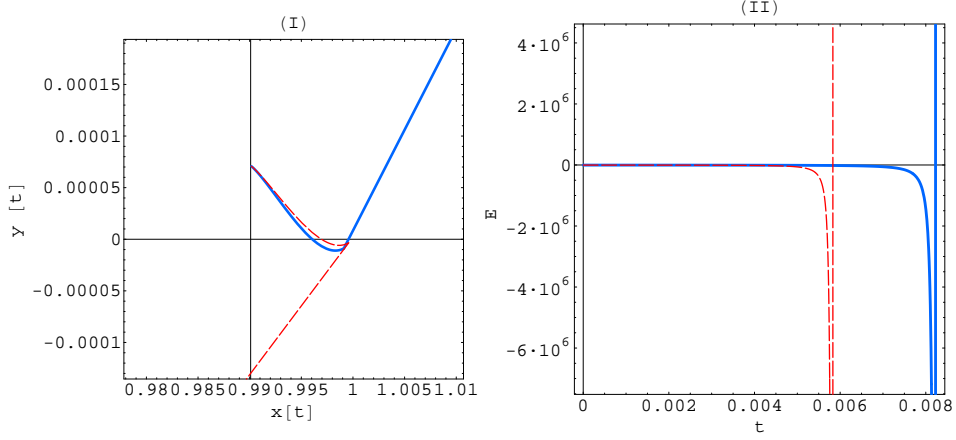


Figure 6: Effect of oblateness coefficient A_2 on the stability of L_1 panel (I) trajectory (II) energy of perturbed point L_1 in which blue solid curves for $A_2 = 0.25$, red curves for $A_2 = 0.50$

the stability regions are affected by the radiation pressure, the oblateness of the second primary and mass of the belt.

6. Acknowledgements

I wish to express my sincere thanks to the Director, Indian School of Mines Dhanbad, the Head of the Department of Applied Mathematics for providing all necessary research facilities in the Department. I also thanks to Professor B. Ishwar, B.R.A. Bihar University Muzaffarpur, all my colleagues and special thanks to Dr. P.S. Rao for the valuable comments and suggestions during the preparation of this article.

References

- [1] V. Szebehely, Theory of orbits. The restricted problem of three bodies, New York: Academic Press, 1967.
- [2] R. W. Farquhar, Journal of Spacecraft and Rockets 4 (1967) 1383–1384.
- [3] R. W. Farquhar, Astronautics Aeronautics (1969) 52–56.

- [4] R. Farquhar, D. Muhonen, L. C. Church, *Journal of the Astronautical Sciences* 33 (1985) 235–254.
- [5] V. Domingo, B. Fleck, A. I. Poland, *Sol. Phys.* 162 (1995) 1–37.
- [6] S. V. Chermnykh, *Vest. Leningrad Mat. Astron.* 2 (1987) 73–77.
- [7] I. Jiang, L. Yeh, *International Journal of Bifurcation and Chaos* 14 (2004) 3153–3166.
- [8] K. E. Papadakis, *Ap&SS* 299 (2005) 67–81.
- [9] I.-G. Jiang, L.-C. Yeh, *Ap&SS* 305 (2006) 341–348.
- [10] L.-C. Yeh, I.-G. Jiang, *Ap&SS* 306 (2006) 189–200.
- [11] K. E. Papadakis, S. S. Kanavos, *Ap&SS* 310 (2007) 119–130.
- [12] I.-G. Jiang, L.-C. Yeh, *Ap&SS* 305 (2006) 341–348.
- [13] M. Miyamoto, R. Nagai, *PASJ* 27 (1975) 533–543.
- [14] B. S. Kushvah, *Ap&SS* (2008) 191–+.
- [15] B. S. Kushvah, *Ap&SS* 323 (2009) 57–63.
- [16] E. A. Grebennikov, D. Kozak-Skoworodkin, *Computational Mathematics and Mathematical Physics* 47 (2007) 1477–1488.
- [17] B. S. Kushvah, *Research in Astronomy and Astrophysics* 9 (2009) 1049–1060.